Mater. Res. Soc. Symp. Proc. Vol. 892 © 2006 Materials Research Society 0892-FF31-03.1

High Degree of Crystalline Perfection in Spontaneously Grown GaN Nanowires*

K. A. Bertness,[1] J. B. Schlager,[1] N. A. Sanford,[1] A. Roshko,[1] T. E. Harvey,[1] A. V. Davydov,[2] I. Levin,[2] M. D. Vaudin,[2] J. M. Barker,[1] P. T. Blanchard,[1] and L. H. Robins[2]
[1]National Institute of Standards and Technology, Boulder, CO 80305, U.S.A.
[2]National Institute of Standards and Technology, Gaithersburg, MD 20899, U.S.A.

ABSTRACT

We have grown a variety of isolated GaN nanowires using gas-source molecular beam epitaxy (MBE) and characterized their structural and optical properties. The nanowires have demonstrated a number of promising materials characteristics, including low defect density and high luminescence intensity. Well separated nanowires formed spontaneously on Si(111) substrates after deposition of a thin AlN buffer layer. Metal catalysts were not used. X-ray diffraction indicates that the *c* and *a* lattice parameters are within 0.01 % of the lattice parameters of bulk GaN. Transmission electron microscopy (TEM) revealed the nanowires to be free of dislocations and stacking faults, although a GaN matrix layer growing at the base of the wires was found to have a high density of basal plane stacking faults. The room temperature photoluminescence (PL) intensity compared favorably with a free-standing film of high quality GaN. Several features of the low temperature PL spectra also indicated that the nanowires had few structural defects or chemical impurities. Finally, electrical characterization of dispersed nanowires demonstrated that efficient electrical contacts could be made and that the resistivity of the nanowires was comparable to that of bulk material.

INTRODUCTION

GaN nanowire growth has been achieved with a number of different methods, including catalyst-based vapor phase growth[1,2], hydride vapor phase epitaxy (HVPE) [3,4], catalyst-based organometallic vapor phase epitaxy, and non-catalyst molecular beam epitaxy[5-8]. The nanowire growth mode is in many ways an extreme extension of epitaxial lateral overgrowth, a method widely used to reduce defect densities for device-quality material in an epitaxial system where high-quality, lattice-matched substrates are not readily available. In this paper, we show that GaN nanowires grown by MBE exhibit a high degree of crystalline perfection through both their structural and optical properties. The properties imply great promise for device applications in which heterostructure strain and residual dislocation density are limiting efficiency and yield. GaN nanowire lasers,[9] light-emitting diodes,[1,10,11] and transistors[2] are among early technological demonstrations emerging from these structures.

EXPERIMENTAL DETAILS

The GaN nanowires were grown on Si(111) substrates in a conventional molecular beam epitaxy growth system with elemental Ga, Al and Si sources and a plasma-assisted nitrogen source. The substrates were cleaned with 1:10 HF:H_2O immediately prior to loading in the growth system, and a thin AlN buffer layer was grown before initiating nanowire growth. High nitrogen flux

(typical beam equivalent pressure[BEP] of 3 x 10^{-3} Pa) and low Ga flux (typical BEP of 1.5 x 10^{-5} Pa) were used to nucleate and sustain nanowire growth at substrate temperatures in the range of 810 °C to 830 °C, as measured by an optical pyrometer. No metal catalysts were used. These conditions are qualitatively similar to but quantitatively different from conditions reported by other growers for nanostructure growth. Further details of the growth process can be found in Ref.[8]. X-ray diffraction data were acquired with a triple-axis diffractometer with a hybrid x-ray mirror and 4-bounce Ge(220) monochromator on the incident beam and channel-cut Ge analyzer crystal with an acceptance angle of 0.0033° on the detector. (The analyzer crystal was not used for rocking curve measurements.) PL data were taken at both room temperature and approximately 3 K with a HeCd laser as an excitation source operating at 325 nm (3.81 eV). The wires were also dispersed onto new substrates for further analysis and electrical contact formation. The dispersal process consisted of ultrasonic agitation of a piece of as-grown wafer in a solvent (such as isopropanol) to remove the wires from the substrate, transfer of the nanowire-solvent mixture to the new substrate with a pipette, and evaporation of the solvent. Nanowires so transferred usually adhered well enough to the substrates to persist through photolithographic processing.

DISCUSSION

Typical GaN nanowires are illustrated with scanning electron microscopy (SEM) images in Fig. 1. Diameters varied from 50 nm to 500 nm in diameter, maintaining nearly constant hexagonal cross-section for an individual wire for lengths up to at least 6.5 μm. The central axis was parallel to the [0001] crystal direction, the *c* axis of the hexagonal GaN crystal structure. As can be seen in Fig. 1(b), the sidewalls of the nanowires were aligned to one another, and x-ray diffraction revealed that the GaN $\langle 1\,1\,\bar{2}\,0 \rangle$ directions were aligned with the Si $\langle 1\,\bar{1}\,0 \rangle$

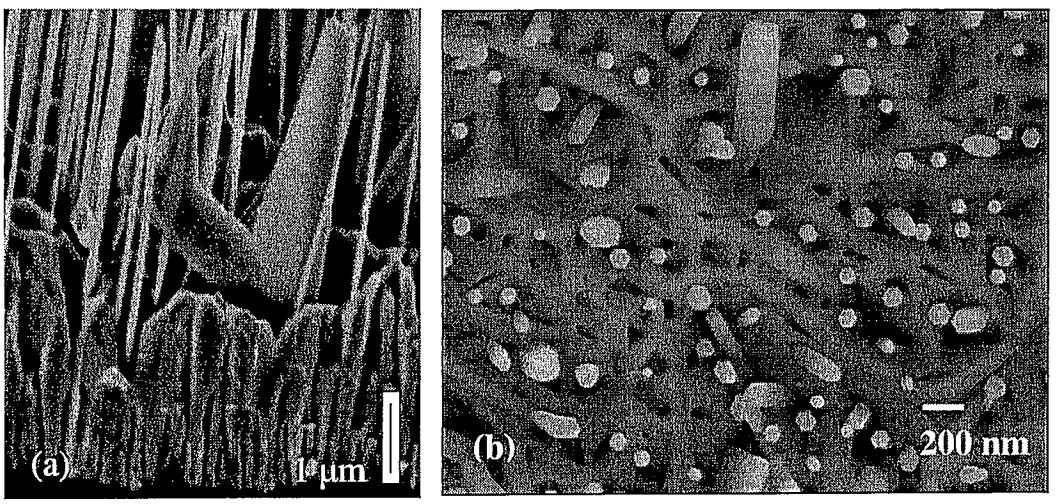

Figure 1. SEM images of long and short nanowire specimens. (a) B738, taken at a tilt of 45° from specimen normal, showing details of the matrix layer and a larger V-shaped fin structure. (b) Plan view of B724, showing hexagonal cross-sections of small wires.

directions. This crystal registration was the same as that observed for thin film growth of GaN on Si[12]. Comparison of the sidewalls with the flat on the Si wafer indicated that the sidewalls conformed to GaN $\{10\bar{1}0\}$ planes. Larger structures ("fins") resembling ribbons or V-shapes were also observed growing at various angles tilted relative to the substrate normal (Fig. 1a). Electron backscatter diffraction (EBSD) on dispersed fins indicated that these structures also grow with the *c*-axis parallel to the crystal edge, even when that edge is not aligned with the substrate normal. In a V-shaped fin, two separate crystals grew out from the base. Wire growth was accompanied by growth of an irregular matrix layer at the base with deep holes, often with faceted sides. Wires appeared to inhibit the growth of the matrix in their immediate vicinity, most likely by consuming available material. The relatively high uniformity of wire lengths suggest that nucleation occurred simultaneously, probably early in the growth, and wires extending from the substrate interface were also observed in cross-sectional TEM images. With field-emission SEM (FESEM), we occasionally observed nucleation of nanowires on top of the matrix layer or other larger structures as well as the intersection of a nanowire with a fin. Adding Be at concentrations of about 10^{19} to 10^{20} cm^{-3} changed the morphology significantly[13], with most of the film consisting of vertical fins or ribbons and very little matrix layer at the base. Doping with Si appeared to have no effect on the growth morphology.

We have previously shown with cross-sectional TEM that the hexagonal nanowires do not contain structural defects of any type, while the matrix layer has a high density of basal plane stacking faults[8]. Basal plane dislocations (not stacking faults) were observed in the larger structures that form in the Be-doped growths (B739), and more extensive dislocation networks occurred where nanowires merged. With these exceptions, the crystalline quality of the nanowires appeared to be perfect. Because nanowires require very little thinning for TEM imaging, a significant fraction of each nanowire is being probed in the images. This low dislocation density has been achieved on Si substrates, whose *a* lattice parameter for the observed crystal alignment is 0.3840 nm, which is ~17 % larger than that of GaN.

To further analyze the crystal structure of the films and nanowires, we collected x-ray diffraction data on a variety of as-grown films, typically acquiring the symmetric diffractions at (0002), (0004), (0006), and the asymmetric diffractions of $(10\bar{1}4)$, $(10\bar{1}5)$ and $(20\bar{2}4)$. The *a* and *c* lattice parameters derived from these data are given in Table I, along with literature values[14,15] for bulk GaN and the FWHM for rocking curves of the (0002) diffraction. The most striking feature of these data is that the lattice parameters for essentially all types of structures were very near to the bulk, relaxed values. With the exception of the short nanowire specimen (B724), it was not possible to distinguish separate peaks for the nanowire contribution and the matrix layer contribution. The *a* lattice parameters were slightly larger for the nanowires and matrix layers than those for bulk GaN, with the separated matrix layer for B724 showing a larger effect. These shifts are consistent with in-plane biaxial tensile strain generated during cooling from growth due to thermal expansion mismatch. Similar thermoelastic strain effects have been observed in ZnO nanowires[16]. The complete relaxation of the crystal structure without extended dislocations is consistent with the TEM data in Ref. [17]. In that work, dislocations in GaN nanowires were confined to within a few nanometers of the nucleation site, and dislocations in matrix layers bent toward the faceted surfaces and therefore did not propagate to the tips of the matrix.

A number of features in the PL data also indicated that the nanowires were of high optical quality, i.e., had low defect densities. As previously published, the room-temperature PL intensity at the band gap from as-grown nanowire samples was frequently stronger than the PL

Table I. Lattice parameters for nanowire (NW) specimens and the matrix layers, compared with bulk GaN, and FWHM of rocking curves (RC) for the (0002) diffraction. The literature data for Si-doped GaN was derived from films that contained some residual strain, which in part accounts for the large *c* parameter and small *a* parameter. The expanded uncertainties for data from this work were approximately 0.000 05 nm for *c*, 0.000 10 nm for *a*, and 0.000 02 nm^3 for a^2c, and include both spatial variations in the specimens as well as instrument precision.

Specimen Name and Description	(0002) RC FWHM (°)	Lattice parameter *c* (nm)	Lattice parameter *a* (nm)	Lattice volume a^2c (nm^3)
Bulk, undoped [14]	-	0.518 46	0.318 76	0.052 68
Bulk, Si-doped [15]	-	0.518 73	0.318 37	0.052 58
B724, 3 μm NWs	0.5	0.518 53	0.318 93	0.052 75
B724, matrix	0.5	0.518 33	0.319 24	0.052 83
B738, 6 μm NWs	0.26	0.518 46	0.318 98	0.052 75
B769, Si-doped NWs	0.25	0.518 39	0.318 86	0.052 71
B771, matrix only	0.21	0.518 46	0.318 92	0.052 73
B739, Be-doped NWs	0.65	0.518 38	0.318 91	0.052 72
B743, Be-doped NWs	0.20	0.518 48	0.318 95	0.052 74

intensity from free-standing GaN films grown by HVPE. A typical low-temperature PL spectrum from a single nanowire is plotted in Fig. 2. The spectrum was dominated by the donor-bound exciton D^0-X_A at 3.472 eV, the strain-free energy position for this peak. The free exciton transitions X_A and X_B were also present. There was little or no donor-to-acceptor (DAP) emission and no yellow luminescence, both signs that few native vacancy defects and chemical impurities were present. The LO-phonon replica peaks were visible even in single nanowire spectra, and a second phonon replica peak set was observed in PL from clumps of nanowires.

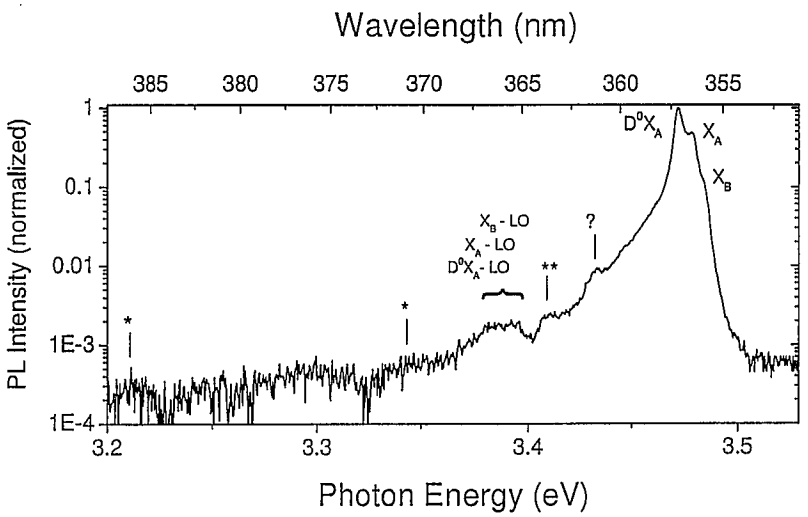

Figure 2. Low-temperature PL spectrum for a single dispersed GaN nanowire. The dominant peak is a donor-bound exciton at 3.472 eV. Additional features are discussed in the text.

Weak peaks(marked with "*") appeared at energies similar to those associated with surface states in Ref [18]. The luminescent output at room temperature was sometimes suppressed after thermal cycling, and this change is currently believed to be due to condensation of impurities on the nanowire surfaces from residual gases in the cryostat.

Finally, initial measurements of the resistance of GaN nanowires suggest that the mobility and doping concentrations of the wires were comparable to those of device-quality GaN. Fig. 3 gives the current-voltage curves for several Si-doped nanowires from a run where the typical nanowire diameter was from 300 nm to 800 nm. The specimens were prepared by dispersal onto quartz substrates followed by oxygen plasma cleaning and deposition of Ti/Al metal pads, with no subsequent annealing. The resistance of the wires varied from 60 kΩ to 150 kΩ, similar to previously published values for GaN nanowires[19,20]. Using 5 μm as the typical length of wires crossing the gap between pads and ignoring any possible contact resistivity, an upper limit to the resistivity of the wires was estimated to be about 0.3 Ω·cm. This value in turn is similar to bulk GaN resistivities[21] of 0.08 Ω·cm for carrier concentration $n = 3 \times 10^{17}$ cm^{-3} and mobility 250 cm^2/V. This rough calculation is not definitive without an independent measurement of mobility, but it does confirm that the nanowires were of reasonably good electrical quality.

CONCLUSIONS

The optical and structural properties of GaN nanowires show that these materials have a high degree of crystalline perfection. X-ray diffraction measurements indicated fully relaxed crystal structures, with no dislocations extending into the nanowires, as determined by TEM. PL intensity at room temperature compared favorably with that of conventionally grown GaN material. The nanowire luminescence spectrum was also free of the yellow and blue broad bands that are commonly observed in thin-film and bulk-like GaN samples, and are usually ascribed to vacancy-type defects and/or chemical impurities. Electrical contacts made to individual nanowires demonstrated that both electrical and optical stimulation of the nanowires is possible. GaN nanowires, because of their ultralow defect content, are therefore excellent candidates for optoelectronic devices such as lasers and for high-power electronics.

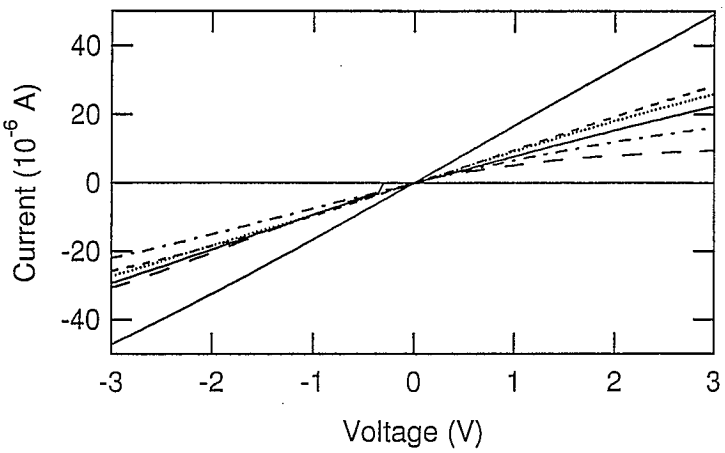

Figure 3. Current-voltage data for Si-doped GaN nanowires. The resistances represented in these curves vary from 60 kΩ to 150 kΩ.

REFERENCES

1. F. Qian, Y. Li, S. Gradecjak, D. Wang, C. J. Barrelet, and C. M. Lieber, *Nano Lett.* **4,** 1975 (2004).
2. M. C. McAlpine, R. S. Friedman, S. Jin, K.-H. Lin, B. Wang, W. U., and C. M. Lieber, *Nano Lett.* **3,** 1531 (2003).
3. G. Seryogin, I. Shalish, W. Moberlychan, and V. Narayanamurti, *Nanotechnology* **16,** 2941–2953 (2005).
4. H. M. Kim, D. S. Kim, Y. S. Park, D. Y. Kim, T. W. Kang, and K. S. Chung, *Adv. Materials* **14,** 991 (2002).
5. J. Ristic, E. Calleja, M. A. Sanchez-Garcia, J. M. Ulloa, J. Sanchez-Paramo, J. M. Calleja, U. Jahn, A. Trampert, and K. H. Ploog, *Phys. Rev. B* **68,** 125305 (2004).
6. J. Ristic, M. A. Sanchez-Garcia, J. M. Ulloa, E. Calleja, J. Sanchez-Paramo, J. M. Calleja, U. Jahn, A. Trampert, and K. H. Ploog, *Phys. Status Solidi B***234,** 717 (2002).
7. A. Kikuchi, M. Kawai, M. Tada, and K. Kishino, *Jpn. J. Appl. Phys. Part 2* **43,** L1524 (2004).
8. K. A. Bertness, N. A. Sanford, J. M. Barker, J. B. Schlager, A. Roshko, A. V. Davydov, and I. Levin, *J. Electron. Mat.* (2006) (in press).
9. J. C. Johnson, H.-J. Choi, K. P. Knutsen, R. D. Schaller, P. Yang, and R. J. Saykally, *Nature Materials* **1,** 106 (2002).
10. Z. Zhong, F. Qian, D. Wang, and C. M. Lieber, *Nano Lett.* **3,** 343 (2003).
11. H.-M. Kim, Y.-H. Cho, H. Lee, S. I. Kim, S. R. Ryu, D. Y. Kim, T. W. Kang, and K. S. Chung, *Nano Lett.* **4,** 1059 (2004).
12. R. Liu, F. A. Ponce, A. Dadgar, and A. Krost, *Appl. Phys. Lett.* **83,** 860 (2003).
13. K. A. Bertness, A. Roshko, N. A. Sanford, J. M. Barker, and A. V. Davydov, *J. Cryst. Growth* (2005) (in press).
14. S. Porowski, *J. Cryst. Growth* **190,** 153 (1998).
15. L. T. Romano, C. G. Van de Walle, J. W. Ager, III, W. Götz, and R. S. Kern, *J. Appl. Phys.* **87,** 7745 (2000).
16. I. Levin, A. Davydov, B. Nikoobakht, N. A. Sanford, and P. Mogilevsky, *Appl. Phys. Lett.* **87,** 103110 (2005).
17. A. Trampert, J. Ristic, U. Jahn, E. Calleja, and K. H. Ploog, in *Microscopy Of Semiconducting Materials 2003*; *Vol. 180* (IOP Publishing Ltd, Bristol, 2003), p. 167.
18. M. A. Reshchikov and H. Morkoç, *J. Appl. Phys.* **97,** 061301 (2005).
19. E. Stern, G. G Cheng, E. Cimpoiasu, R. Klie, S. Guthrie, J. Klemic, I. Kretzschmar, E. Steinlauf, D. Turner-Evans, E. Broomfield, J. Hyland, R. Koudelka, T. Boone, M. Young, A. Sanders, R. Munden, T. Lee, D. Routenberg, and M. A. Reed, *Nanotechnology* **16,** 2941–2953 (2005).
20. S. Han, W. Jin, D. Zhang, T. Tang, C. Li, X. Liu, Z. Liu, B. Lei, and C. Zhou, *Chemical Physics Letters* **389,** 176 (2004).
21. J. T. Torvik, in *III-V Nitride Semiconductors: Electrical, Structural and Defects Properties*, edited by M. O. Manasreh (Elsevier Science B. V., Amsterdam, 2000), p. 17.